ARL-TN-1296 ● JAN 2026

# Preparation of Free-Standing Metallographic Samples for High-Throughput Characterization

by Clinton J. Strosser, Nathaniel Rorer, and Brady G. Butler

## NOTICES

### Disclaimers

The findings in this report are not to be construed as an official Department of the Army position unless so designated by other authorized documents.

Citation of manufacturer's or trade names does not constitute an official endorsement or approval of the use thereof.

Destroy this report when it is no longer needed. Do not return it to the originator.

ARL-TN-1296 ● JAN 2026


# Preparation of Free-Standing Metallographic Samples for High-Throughput Characterization

**Clinton J. Strosser and Nathaniel Rorer**
*Texas A&M University*

**Brady G. Butler**
*DEVCOM Army Research Laboratory*

# REPORT DOCUMENTATION PAGE

| 1. REPORT DATE | 2. REPORT TYPE | 3. DATES COVERED | |
|---|---|---|---|
| | | START DATE | END DATE |
| January 2026 | Technical Note | 1 January 2024 | 31 December 2025 |

**4. TITLE AND SUBTITLE**
Preparation of Free-Standing Metallographic Samples for High-Throughput Characterization

| 5a. CONTRACT NUMBER | 5b. GRANT NUMBER | 5c. PROGRAM ELEMENT NUMBER |
|---|---|---|
| W911NF-22-2-0106 | | |
| **5d. PROJECT NUMBER** | **5e. TASK NUMBER** | **5f. WORK UNIT NUMBER** |
| | | |

**6. AUTHOR(S)**
Clinton J. Strosser, Nathaniel Rorer, and Brady G. Butler

**7. PERFORMING ORGANIZATION NAME(S) AND ADDRESS(ES)**
DEVCOM Army Research Laboratory
ATTN: FCDD-RLA-MF
Aberdeen Proving Ground, MD 21005

**8. PERFORMING ORGANIZATION REPORT NUMBER**
ARL-TN-1296

| 9. SPONSORING/MONITORING AGENCY NAME(S) AND ADDRESS(ES) | 10. SPONSOR/MONITOR'S ACRONYM(S) | 11. SPONSOR/MONITOR'S REPORT NUMBER(S) |
|---|---|---|
| | | |

**12. DISTRIBUTION/AVAILABILITY STATEMENT**
DISTRIBUTION STATEMENT A. Approved for public release: distribution unlimited.

**13. SUPPLEMENTARY NOTES**
ORCIDs: Clinton Strosser, 0009-0007-8388-1948; Nathaniel Rorer, 0009-0001-5561-4750; Brady G. Butler, 0000-0002-7677-9685

**14. ABSTRACT**
High-quality, free-standing metallographic specimens have remained challenging to produce in laboratories that rely on rapid, multi-technique characterization. Conventional epoxy or phenolic resin mounts simplify handling but frequently interfere with electron microscopy and mechanical testing, where coplanarity, electrical grounding, and mechanical stiffness are critical. In this work, an efficient procedure was developed for creating free-standing metallographic mounts using thermoplastic adhesives, with specific attention given to surface alignment, adhesion strength, and ease of removal. The method was designed to support high-throughput testing pipelines in which specimens must be prepared, characterized, and reprocessed in rapid succession. Emphasis was placed on adhesive selection, temperature control, and mitigation of entrapped air to preserve surface integrity for techniques including electron backscatter diffraction, nanoindentation, Vickers hardness testing, and micro-impact experiments. This approach provided a reproducible and adaptable pathway for producing polished, mechanically stable, and reworkable specimens suitable for advanced metallographic studies.

**15. SUBJECT TERMS**
mounting, polishing, high-throughput characterization, electron backscatter diffraction, EBSD, nanoindentation, Sciences of Extreme Materials

| 16. SECURITY CLASSIFICATION OF: | | | 17. LIMITATION OF ABSTRACT | 18. NUMBER OF PAGES |
|---|---|---|---|---|
| a. REPORT | b. ABSTRACT | C. THIS PAGE | | |
| UNCLASSIFIED | UNCLASSIFIED | UNCLASSIFIED | UU | 25 |

| 19a. NAME OF RESPONSIBLE PERSON | 19b. PHONE NUMBER *(Include area code)* |
|---|---|
| Brady G. Butler | (520) 691-5844 |

**STANDARD FORM 298 (REV. 5/2020)**
*Prescribed by ANSI Std. Z39.18*

## Contents

## List of Figures

## List of Tables

## Acknowledgments

This research was sponsored in part by the Army Research Laboratory under Cooperative Agreement Number W911NF-22-2-0106. The views and conclusions contained in this document are those of the authors. They should not be interpreted as representing the official policies, either expressed or implied, of the Army Research Laboratory or the U.S. Government.

We thank Daniel O. Lewis, Wenle Xu, Jacob Hempel, and Braden L. Miller of Texas A&M University, Department of Materials Science and Engineering, for preparing figures and discussions related to this manuscript.

# 1. Introduction

Metallographic specimens are routinely mounted in epoxy, phenolic resins (e.g., Bakelite), or similar media to improve handling, provide edge retention, and facilitate conventional preparation workflows. While these approaches remain standard practice, many advanced characterization techniques require free-standing specimens with flat, parallel faces and mirror-quality surfaces. Such preparation becomes essential when downstream analyses are sensitive to specimen geometry, compliance, or electrical grounding.

Several high-strain-rate testing methods, including laser-induced projectile impact testing and high-strain-rate nanoindentation, have limited sample size requirements and require highly polished surfaces. Similarly, electron backscatter diffraction (EBSD) may have sample size and geometry limitations but requires deformation-free surfaces to maximize pattern quality and indexing reliability. In these contexts, traditional mounting approaches may introduce artifacts, restrict testing geometries, or hinder high-throughput experimental workflows.[1–3]

In this technical note, a practical procedure was described for producing free-standing metallographic specimens using Crystalbond 509 thermoplastic adhesive. Emphasis was placed on adhesion strength, surface coplanarity, and compatibility with a range of microscale mechanical and microstructural characterization techniques. The procedure was developed to support the ARL program High-Throughput Materials Development for Extreme Conditions (HTMDEC), in which iterative preparation, imaging, and mechanical probing were required to be conducted efficiently while maintaining high data quality.

While thermoplastic mounting adhesives are not new, the present work distinguishes itself by establishing a repeatable, demountable preparation workflow explicitly tailored for high-throughput materials discovery. The procedure emphasizes quantitative planarity control, repeated reuse without surface degradation, and compatibility across scanning electron microscopy (SEM), EBSD, nanoindentation, and high-strain-rate testing modalities.

# 2. Methods, Assumptions, and Procedures

## 2.1 Sample and Puck Preparation

Mounting pucks were machined from a 1.25-inch-diameter 6061 aluminum rod (Figure 1) and sectioned into 1-inch-thick disks. This geometry was selected to ensure compatibility with both the automatic polishing system and the conventional

nanoindenter stage. Prior to mounting, both the puck and specimen were thoroughly degreased using acetone or ethanol. Specimens were subsequently placed in an ultrasonic cleaner for 10 min to remove residual surface contamination. Complete drying of all surfaces was required to ensure adequate adhesive bonding.

**Figure 1. Example of proper fitment for a 3D-printed Crystalbond retaining ring mounted onto an aluminum puck.**

The mounting adhesive, Crystalbond, was frequently stored under refrigerated conditions to increase brittleness and facilitate sectioning. Small portions of adhesive were removed using a razor blade and collected for application. This approach allowed controlled dosing and reduced the likelihood of entrapped air during melting.

## 2.2 Preheating the Puck

The mounting puck was heated using a temperature-controlled hot plate or heat gun, as illustrated in Figure 2. Manufacturer-recommended temperature limits were not exceeded to avoid adhesive degradation. Prior to heating, a 3D-printed retaining ring was affixed to the puck. This ring served to contain the molten adhesive and to shield sharp specimen edges from contacting and damaging polishing pads during subsequent grinding and polishing steps. It was noted that additively manufactured retaining rings may exhibit surface porosity, which can trap abrasive particles and contribute to carryover during polishing. This effect was mitigated by printing thin-walled ring geometries and thoroughly cleaning between preparation steps.

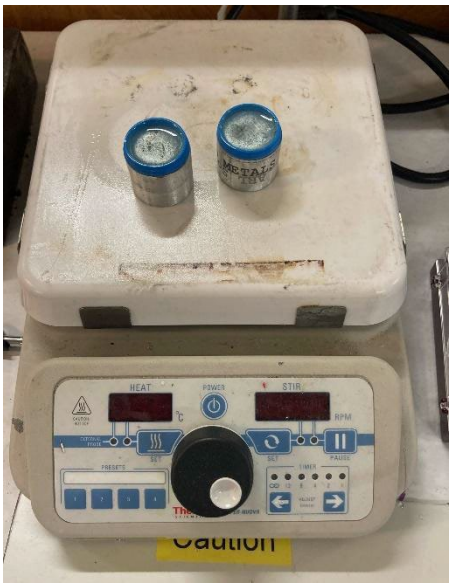


**Figure 2. Hot plate setup used for heating Crystalbond on an aluminum puck mount.**

## 2.3 Melting and Applying Crystalbond

Crystalbond was applied to the heated puck by incrementally depositing small portions into the center of the retaining ring until a uniform molten pool was formed (Figure 3). The adhesive was distributed evenly to fully surround the specimen and fill the mounting cavity. The adhesive level was maintained slightly above the specimen surface to accommodate material removal during grinding.


**Figure 3. Commercial Crystalbond 509 mounting adhesive supplied in cylindrical geometry, allowing controlled sectioning and repeatable dosing during mounting.**

Crystalbond 509 (Table 1) was selected for this work due to its moderate bonding strength, relatively low softening temperature, and clean solvent release in acetone, which facilitated repeated mounting and demounting cycles.

**Table 1. Properties of Crystalbond 509 thermoplastic mounting adhesive.**

| Property | Value |
|---|---|
| Appearance | Clear |
| Solvent for removal | Acetone |
| Available geometry (round) | 0.875 inch (22.2 mm) diameter × 7 inches (178 mm) long |
| Flow/melting temperature | 121 °C (250 °F) |
| Softening temperature | 71 °C (159.8 °F) |
| Viscosity at flow temperature | 6000 cP |
| Mass per cylinder | ~0.2 lb (90 g) |

Although Crystalbond 509 was selected for the present study, alternative thermoplastic adhesives may be appropriate depending on specimen geometry and downstream processing constraints. Higher-temperature adhesives can improve stability during extended polishing or ion milling, whereas stronger formulations may be advantageous for larger or mechanically robust specimens. Conversely, lower-temperature adhesives may be preferred for fragile or thermally sensitive materials.

In practice, adhesive selection was governed by three primary considerations:

- Softening temperature relative to the preparation process
- Bonding strength and specimen geometry
- Ease of release relative to downstream analysis requirements

## 2.4 Mounting the Sample

The specimen was gently inserted into the molten adhesive and positioned to ensure central alignment and surface levelness. Care was taken to avoid entrapping air bubbles, as voids may trap abrasive particles and introduce contamination during polishing. Representative mounting states before and after specimen insertion are shown in Figure 4.

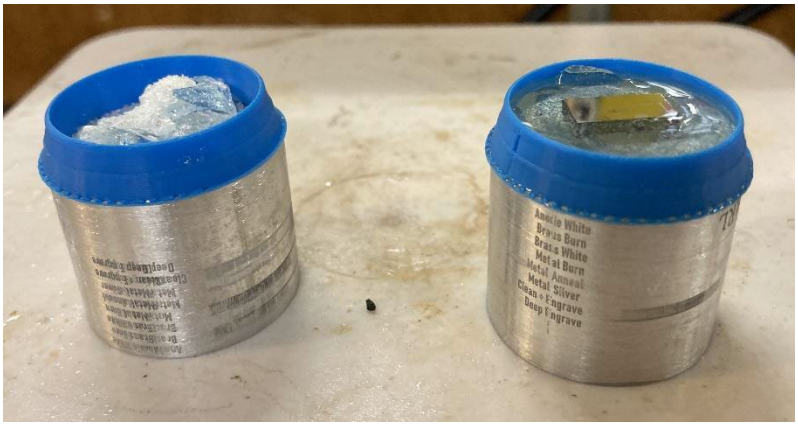

**Figure 4. Sample showing solid Crystalbond shards portioned into a retaining ring (left) and a mounted specimen prior to cooling (right).**

## 2.5 Building an Adhesive Fillet

An adhesive fillet was constructed around the specimen perimeter, as shown in Figure 5, to provide additional mechanical support during grinding. This fillet reduced the likelihood of specimen rocking or detachment under applied polishing loads.

**Figure 5. Overhead view of molten Crystalbond surrounding a copper specimen prior to cooling.**

Figure 6 shows a schematic illustration of sample mounting on an aluminum puck using Crystalbond without a retaining ring. In this configuration, adhesion and mechanical stability were provided by the surface tension of the molten Crystalbond and the formation of a continuous adhesive fillet around the specimen perimeter. This approach was sufficient for low-profile specimens, where the adhesive fillet fully encapsulated sharp edges and reduced the risk of polishing pad damage. However, taller specimens were more difficult to stabilize using surface tension alone, increasing the likelihood of exposed edges that could abrade or tear polishing pads during grinding and polishing operations.

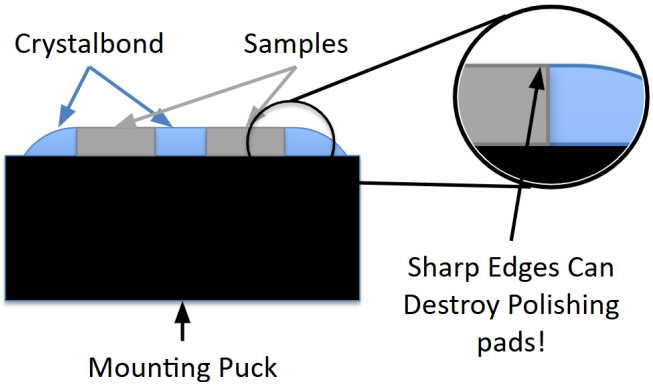


**Figure 6. Schematic illustration of Crystalbond mounting without an adhesive retaining ring, where specimen adhesion and mechanical stability are provided by surface tension of the molten adhesive and the formation of a continuous fillet around the specimen perimeter.**

## 2.6 Cooling and Solidification

The mounted puck was allowed to cool undisturbed at room temperature. Crystalbond hardened rapidly upon removal from heat. The mount was visually inspected to confirm complete adhesion and the absence of visible voids or bubbles.

## 2.7 Final Inspection Prior to Grinding

Prior to grinding, the specimen surface was verified to be slightly recessed relative to the surrounding adhesive. This configuration ensured that excess adhesive would be removed during the initial grinding step. Surface flatness and uniformity were required to prevent edge rounding or polishing pad damage.

## 2.8 Grinding

Grinding was initiated using 320-grit silicon carbide paper, followed by 600-grit paper, as summarized in Table 2. Water was used for lubrication to minimize frictional heating. Grinding was continued until the specimen and adhesive surfaces were co-planar and perpendicular to the puck axis. A representative sample after grinding operations is shown in Figure 7.

**Table 2. Sample preparation data for grinding procedure.**

| Grinding grit size | Pad type | Pad pressure (lbf) | Time per process (min) |
|---|---|---|---|
| 320 grit | Sandpaper | 5 | 2 |
| 600 grit | Sandpaper | 5 | 3 |

.

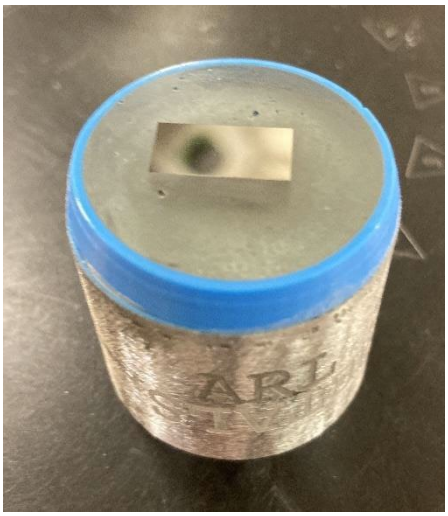

**Figure 7. Sample between polishing steps, showing surface coplanarity and the emergence of intrinsic porosity following adhesive removal.**

## 2.9 Polishing

Polishing was conducted sequentially using 9-, 3-, and 0.04-µm abrasives according to Table 3. After each polishing step, specimens were rinsed with tap water and cleaned using a mild detergent, followed by ultrasonic cleaning to prevent abrasive carry-over. In cases where polishing resulted in a dull surface finish, an additional attack polish using hydrogen peroxide was applied as needed. Polishing times were adjusted based on material response.

**Table 3. Sample preparation data for polishing procedure.**

| Polishing grit size | Pad type | Pad pressure (lbf) | Time per process (min) |
|---|---|---|---|
| 9-µm grit | Goldlabel | 5 | 6 |
| 3-µm grit | Dia Mat | 5 | 6 |
| 0.04-µm grit | Final A | 5 | 12 |

.

Vibratory polishing using a VibroMet 2 system (Figure 8) was employed for final surface preparation when SEM imaging was required. A 0.04-µm colloidal silica suspension was used. Extended vibratory polishing was avoided for materials susceptible to silica-induced etching, which can result in faceting and degraded surface roughness.


**Figure 8. VibroMet 2 automatic polisher used for final polishing steps.**

For specimens intended for nanoindentation, preparation targets included a surface tilt less than 1° relative to the indenter axis and an arithmetic roughness value less than 5% of the intended maximum indentation depth. These criteria were later verified using optical profilometry. These polishing procedures are general and may be modified depending on material requirements.

# 3. Results and Discussion

## 3.1 Cleaning and Sample Removal

Following polishing, specimens were rinsed thoroughly with tap water and then with distilled water to produce a streak-free surface suitable for microscopy (Figure 9). Samples were dried using compressed air. When removal from the Crystalbond mount was required, either thermal softening or solvent dissolution was employed. Acetone was effective for removing small adhesive volumes, whereas reheating was more efficient for bulk removal. Care was taken to prevent adhesive transfer onto polished surfaces during demounting.

**Figure 9. Representative copper specimens after final polishing, showing mirror-quality surfaces suitable for high-resolution imaging.**

## 3.2 Imaging

SEM and optical micrographs were acquired to document surface features such as grain size, grain morphology, and deformation structures (Figures 10 and 11). These images served as reference points for iterative comparisons within the HTMDEC workflow. Imaging was conducted using optical microscopy (OM), secondary electron (SE) imaging, backscattered electron (BSE) imaging, and EBSD mapping.

Figure 10 also demonstrates the sensitivity of BSE imaging to surface preparation quality. Initial preparation resulted in selective etching, residual scratches, and polishing compound contamination. Following optimization, surface relief and damage were significantly reduced, producing uniform contrast suitable for high-throughput analysis.

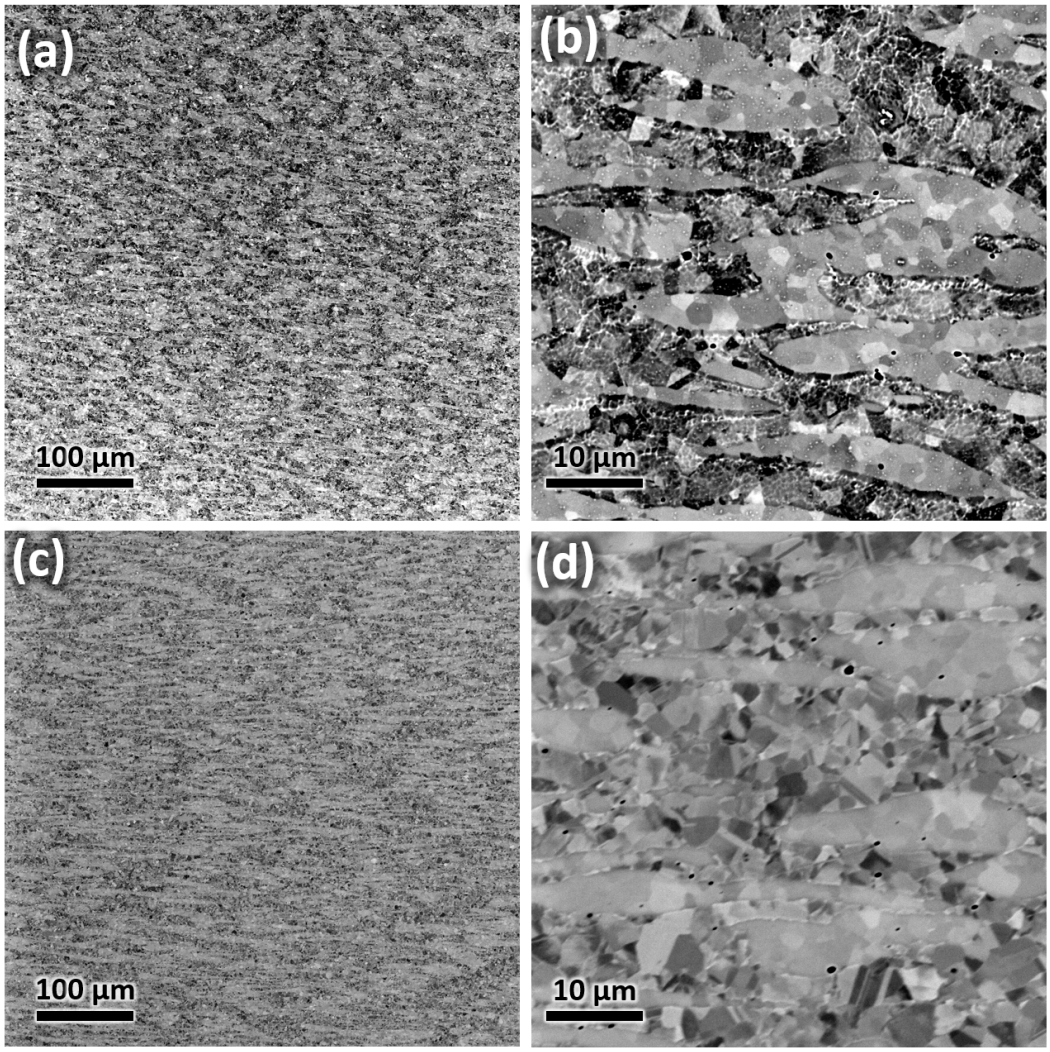


**Figure 10. BSE micrographs of a representative HTMDEC sample (AAD12) illustrating the effect of surface preparation quality. Panels (a) and (b) show the initially prepared condition, where selective etching, residual scratches, and colloidal silica contamination are evident. Panels (c) and (d) show the same material after optimized preparation following the procedures outlined above, exhibiting minimal surface relief, reduced polishing damage, and a uniform contrast suitable for high-resolution imaging and indentation.**

Figure 11 shows multimodal imaging of a properly prepared specimen, including artifact-free BSE images, a high-quality EBSD orientation map, and an SE image confirming the absence of residual polishing or mounting compounds.

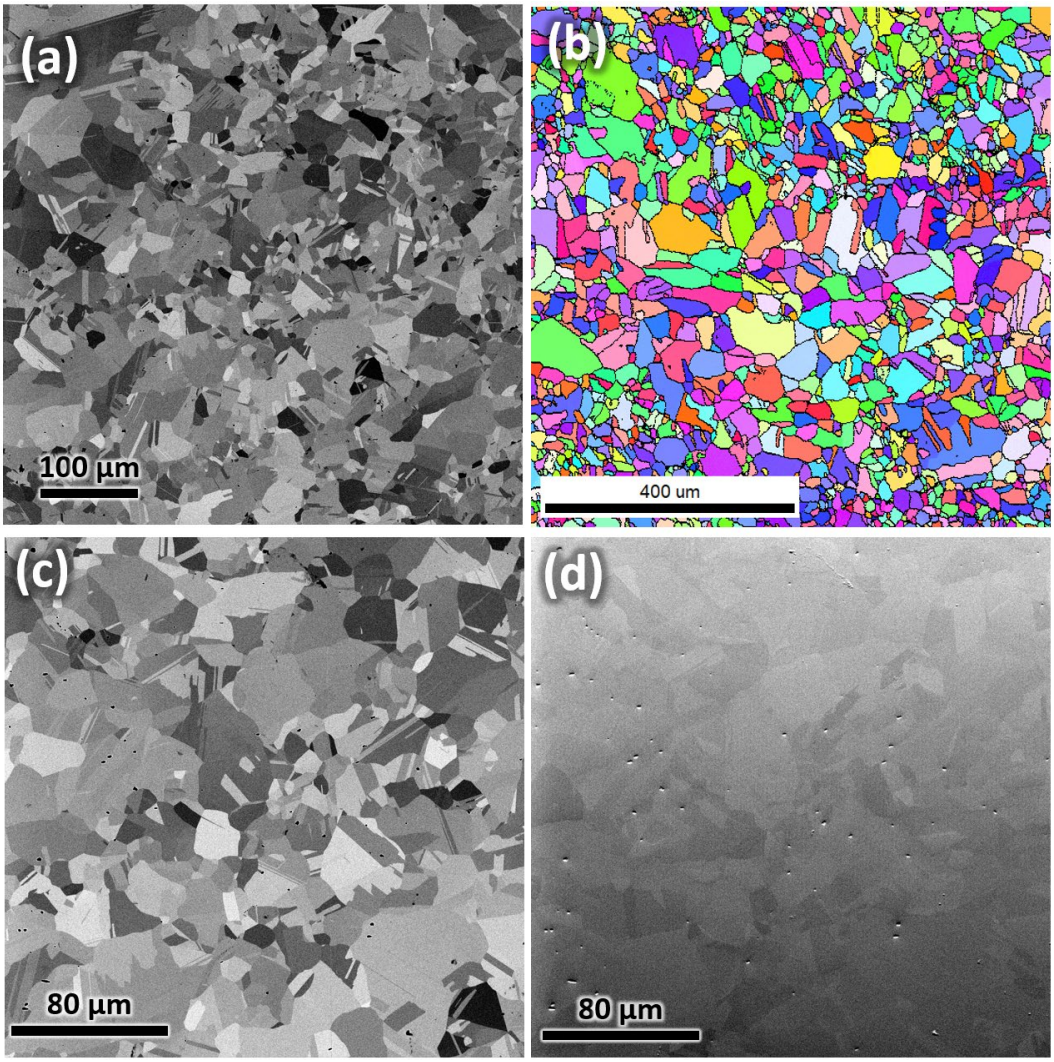


**Figure 11. Multimodal electron microscopy images of a properly prepared HTMDEC sample (CBB12). Backscattered electron images (a, c) show a uniform, artifact-free surface with clear phase and orientation contrast. The corresponding EBSD orientation map (b) demonstrates high indexing quality and continuous grain boundary definition. An SE image (d) confirms minimal surface damage, with no observable residue from colloidal silica polishing or Crystalbond mounting. Intrinsic microstructural features such as porosity remain visible.**

## 3.3 Indentation Preparation

Following the guidelines outlined in the ISO 14577 standard,[4] a mirror-finished, debris-free surface was required for indentation testing with a surface tilt less than 1° normal to the test force direction. Finally, the arithmetic average roughness ($Ra$) was maintained below 5% of the maximum depth ($h$) at which nanoindentation hardness measurements were reported. Alternatively, the planar average roughness, based on a 2D measurement (i.e., $Sa$), was used as the roughness metric. Non-

contact profilometry using a Keyence VK-X1000 3D Surface Profiler was used to confirm surface quality.

Figure 12 illustrates the complementary information provided by SE and BSE imaging during indentation assessment. While SE images confirm that the surface finish is suitable for indentation, BSE images reveal subsurface deformation fields that are not apparent from surface topography alone. These deformation zones can influence the measured mechanical response, particularly in materials with heterogeneous microstructures. Incorporating both imaging modes is therefore critical for interpreting indentation data within a high-throughput framework.

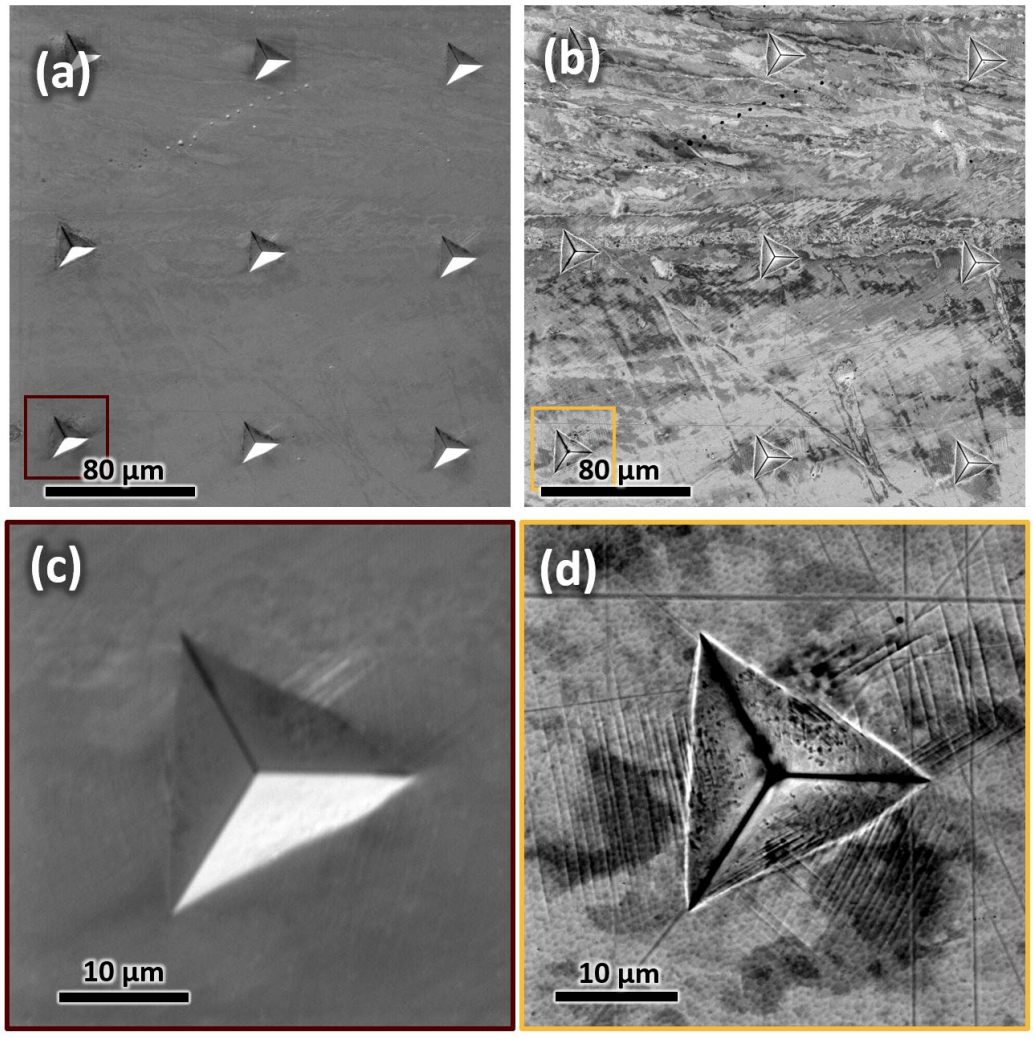


**Figure 12. SE and BSE micrographs of indentation arrays and representative individual indents on a HTMDEC sample (AAD05). Low-magnification SE and BSE images of indentation arrays are shown in (a) and (b), respectively, while higher-magnification views of individual indents are shown in (c) and (d). SE images (a, c) indicate a high-quality surface finish with minimal topographic artifacts. In contrast, BSE images (b, d) reveal significant subsurface deformation and contrast variations surrounding the indents.**

Figure 13 demonstrates the role of optical and profilometric measurements in validating indentation readiness. The low measured inclination angle confirms appropriate specimen alignment relative to the indenter axis, while the quantified surface roughness satisfies established criteria for nanoindentation testing. These measurements provide a quantitative check on preparation quality, complementing electron microscopy observations and ensuring that measured mechanical properties reflect intrinsic material behavior rather than surface artifacts.

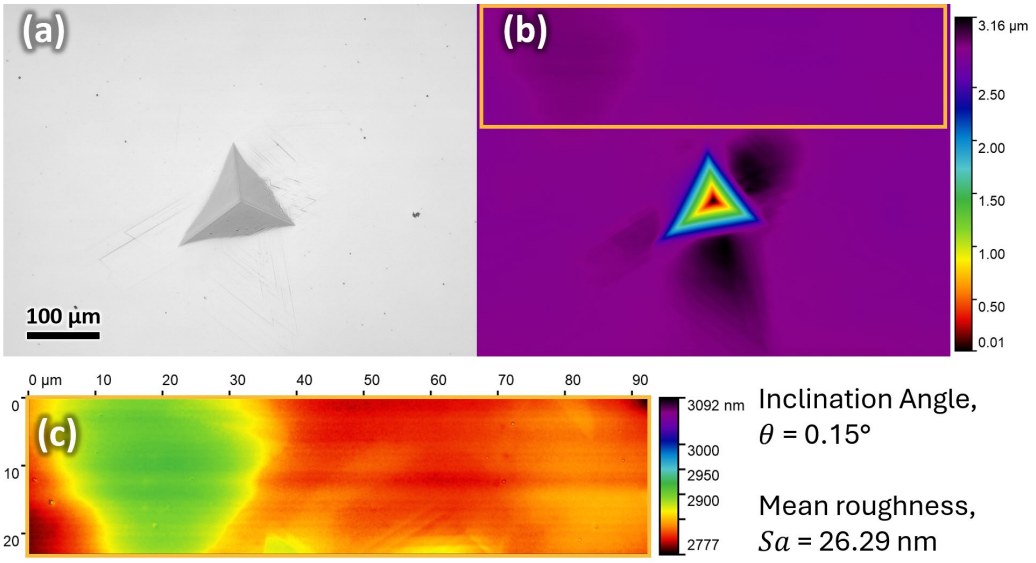


**Figure 13. OM and surface profilometry of an indent on a properly prepared HTMDEC specimen (CBB12). An optical micrograph of the indent is shown in (a). The corresponding height map and line profile obtained by profilometry are shown in (b) and (c), respectively. Note that there is some asymmetry in the indentation profile, but the measured surface inclination angle is well below the 1° threshold. The mean areal roughness (*Sa*) indicates that reliable hardness measurements can be obtained at indentation depths of 525 nm and greater.**

## 4. Conclusions

A systematic procedure was developed for mounting, polishing, demounting, and cleaning metallographic specimens to produce high-quality, free-standing samples suitable for high-throughput materials characterization. Each stage of the workflow was refined to promote mechanical stability, surface planarity, and reproducibility. The use of a 3D-printed retaining ring improved adhesive containment, protected polishing consumables, and enhanced mounting uniformity.

Properly prepared specimens were shown to be essential for generating reliable microstructural and micromechanical data using SEM, EBSD, nanoindentation, and related techniques. Adherence to the described protocol enabled consistent preparation across large specimen sets, supporting statistically meaningful comparisons and robust datasets.

Future refinements should address planarity issues associated with individual-force polishing holders. Adoption of central-force holders is expected to reduce specimen rocking, minimize doming, and improve alignment for nanoindentation arrays. Maintaining total surface deviation below 1.0°, and preferably below 0.5°, was recommended. Verification using optical profilometry was shown to be effective.

In summary, meticulous specimen preparation remains indispensable for modern materials characterization. The workflow presented here reduces experimental scatter, minimizes preparation-induced artifacts, and enables statistically robust comparisons across large specimen sets. Such control is essential for avoiding false structure–property correlations and for realizing the full potential of high-throughput materials discovery platforms.

## 5. References


1. Paramore JD et al. Two-shot optimization of compositionally complex refractory alloys. Acta Mater. 2025;289:120820. https://doi.org/10.1016/J.ACTAMAT.2025.120820

2. Mulukutla M et al. Illustrating an effective workflow for accelerated materials discovery. Integr Mater Manuf Innov. 2024;13:453–473. https://doi.org/10.1007/S40192-024-00357-3

3. Hastings T et al. Accelerated multi-objective alloy discovery through efficient Bayesian methods: application to the FCC high entropy alloy space. Acta Mater. 2025;297:121173. https://doi.org/10.1016/J.ACTAMAT.2025.121173

4. International Organization for Standardization. Metallic materials—instrumented indentation test for hardness and materials parameters. Part 1: Test method. 2015 July. ISO 14577-1:2015.

## List of Symbols, Abbreviations, and Acronyms

| | |
|---|---|
| 2/3D | Two-/Three-Dimensional |
| BSE | Backscattered Electron |
| EBSD | Electron Backscatter Diffraction |
| $h$ | Indentation Depth (Nanoindentation) |
| HTMDEC | High-Throughput Materials Discovery for Extreme Conditions |
| lbf | Pound-Force |
| OM | Optical Microscopy |
| $Ra$ | Linear Arithmetic Average of Roughness |
| $Sa$ | Planar Arithmetic Average of Roughness |
| SE | Secondary Electron |
| SEM | Scanning Electron Microscope |

| | |
|---|---|
| 1 (PDF) | DEFENSE TECHNICAL INFORMATION CTR DTIC OCA |
| 1 (PDF) | DEVCOM ARL FCDD RLB CI TECH LIB |